

High velocity spikes in Gowdy spacetimes

David Garfinkle*

Department of Physics, Oakland University Rochester, Michigan 48309

Marsha Weaver†

Theoretical Physics Institute, University of Alberta Edmonton, AB, Canada T6G 2J1

We study the behavior of spiky features in Gowdy spacetimes. Spikes with velocity initially high are, generally, driven to low velocity. Let n be any integer greater than or equal to 1. If the initial velocity of an upward pointing spike is between $4n - 3$ and $4n - 1$ the spike persists with final velocity between 1 and 2, while if the initial velocity is between $4n - 1$ and $4n + 1$, the spiky feature eventually disappears. For downward pointing spikes the analogous rule is that spikes with initial velocity between $4n - 4$ and $4n - 2$ persist with final velocity between 0 and 1, while spikes with initial velocity between $4n - 2$ and $4n$ eventually disappear.

PACS numbers: 04.20.-q, 04.25.Dm, 04.20.Dw

I. INTRODUCTION

There have been several investigations of the approach to the singularity in inhomogeneous cosmologies, predominantly in the case that a two-dimensional symmetry group acts spatially [1, 2, 3, 4, 5, 6, 7, 8, 9, 10, 11, 12]. The most extensively studied class of such spacetimes is the class of Gowdy spacetimes[13] on $T^3 \times R$. Numerical studies of these spacetimes show that the approach to the singularity is asymptotically velocity term dominated (AVTD) except at an isolated set of points.

As shown in [6] this behavior can be understood by considering certain terms in the equations as “potentials” that affect the dynamics at each spatial point. These potentials drive the dynamics into the AVTD regime, except at those isolated points where one of the potentials vanishes. The behavior at each of these isolated points differs from that of its neighbors, leading to the creation of features called spikes that become narrow as the singularity is approached. The analysis of [6] uses an explicit approximation to find a closed form expression for the behavior of the spikes. However, this approximation only remains valid throughout the approach to the singularity for a certain class of spikes: those for which the “velocity” v of the spike is “low” ($1 < v < 2$ for “upward pointing spikes” and $0 < v < 1$ for “downward pointing spikes”). What then happens if a spike forms and it initially has “high” velocity? Certain terms in the evolution equations which are decaying for low velocity spikes are instead growing in magnitude for a high velocity spike and the sign of the net effect is such that the velocity should decrease [9, 16]. An explicit approximation that is valid as the velocity at a high velocity spike decreases has not been found, leaving open the question, “What is the long term behavior of initially high velocity spikes in Gowdy spacetimes?”

To answer this question, we perform numerical simulations of Gowdy spacetimes with these high velocity spikes. Since the spikes become ever narrower as the singularity is approached, until just this narrowness causes the velocity to decrease if it is originally high, extremely high resolution is needed to follow the detailed behavior of the spike. We use a numerical method that was used in [14] to study critical collapse. Here the equations are put in characteristic form and the outermost grid point is chosen to be the ingoing light ray that hits the singularity at the center of the spike. In this way, the grid gets smaller as the feature that it needs to resolve shrinks.

Section 2 presents the equations and the characteristic numerical method. Results are given in section 3 and conclusions in section 4.

II. EQUATIONS AND NUMERICAL METHODS

The Gowdy metric on $T^3 \times R$ takes the form

$$ds^2 = e^{\lambda/2} t^{-1/2} (-dt^2 + dx^2) + t[e^P(dy + Qdz)^2 + e^{-P}dz^2] \quad (1)$$

*Email: garfinkl@oakland.edu

†Email: mweaver@phys.ualberta.ca

where P , Q and λ are functions of t and x . The vacuum Einstein field equations split into “evolution” equations for P and Q

$$P_{,tt} + t^{-1}P_{,t} - P_{,xx} + e^{2P}(Q_{,x}^2 - Q_{,t}^2) = 0 \quad (2)$$

$$Q_{,tt} + t^{-1}Q_{,t} - Q_{,xx} + 2(P_{,t}Q_{,t} - P_{,x}Q_{,x}) = 0 \quad (3)$$

and “constraint” equations for λ

$$\lambda_{,t} = t[P_{,t}^2 + P_{,x}^2 + e^{2P}(Q_{,t}^2 + Q_{,x}^2)] \quad (4)$$

$$\lambda_{,x} = 2t(P_{,x}P_{,t} + e^{2P}Q_{,x}Q_{,t}) \quad (5)$$

(here $_{,a} = \partial/\partial a$). The constraint equations determine λ once P and Q are known. The integrability conditions for the constraint equations are satisfied as a consequence of the evolution equations. Since the evolution equations do not depend on λ there is essentially a complete decoupling of constraints from evolution equations. Therefore, for the purposes of this paper we will treat only equations (2-3). The only restriction that the constraints place on initial data for equations (2-3) is the following: since λ at $x = 0$ is the same as λ at $x = 2\pi$, it follows that the integral from 0 to 2π of the right hand side of equation (5) must vanish. We require that this restriction is satisfied by the initial data for equations (2-3) and then these equations insure that the restriction is also satisfied at subsequent times.

The singularity is at $t = 0$. It is often helpful to introduce the coordinate $\tau \equiv -\ln t$. Thus the singularity is approached as $\tau \rightarrow \infty$. In terms of this coordinate, the evolution equations (2-3) become

$$P_{,\tau\tau} - e^{2P}Q_{,\tau}^2 - e^{-2\tau}P_{,xx} + e^{2(P-\tau)}Q_{,x}^2 = 0 \quad (6)$$

$$Q_{,\tau\tau} + 2P_{,\tau}Q_{,\tau} - e^{-2\tau}(Q_{,xx} + 2P_{,x}Q_{,x}) = 0 \quad (7)$$

The velocity is defined as $v = \sqrt{P_{,\tau}^2 + e^{2P}Q_{,\tau}^2}$. In the limit of large τ , if we neglect the terms in equations (6-7) proportional to $e^{-2\tau}$ then we find that $v \rightarrow v_\infty$ and $P \rightarrow v_\infty\tau$ where v_∞ depends only on x . However, if $v_\infty > 1$ then neglect of the term $e^{2(P-\tau)}Q_{,x}^2$ is not justified. What happens is that if $P_{,\tau}$ is greater than 1, then this term drives it to values less than 1, except at the isolated points where $Q_{,x} = 0$. At those points upward pointing spikes form. The previous studies [6, 9, 16] suggest that if $1 < P_{,\tau} < 2$ at the spike, the spike will persist, but that if $P_{,\tau} > 2$ at the spike, $P_{,\tau\tau}$ will become negative and its magnitude will start growing exponentially in τ as the spike narrows. But the previous studies leave open the question, “What happens next?” We want to know the outcome.

For our purposes, we will need the field equations in characteristic form. To that end we introduce null coordinates $u \equiv t + x$ and $w \equiv t - x$ and characteristic variables A , B , C and D given by

$$A = (u + w)P_{,w} \quad (8)$$

$$B = (u + w)P_{,u} \quad (9)$$

$$C = (u + w)e^P Q_{,w} \quad (10)$$

$$D = (u + w)e^P Q_{,u} \quad (11)$$

The evolution equations (2-3) then become

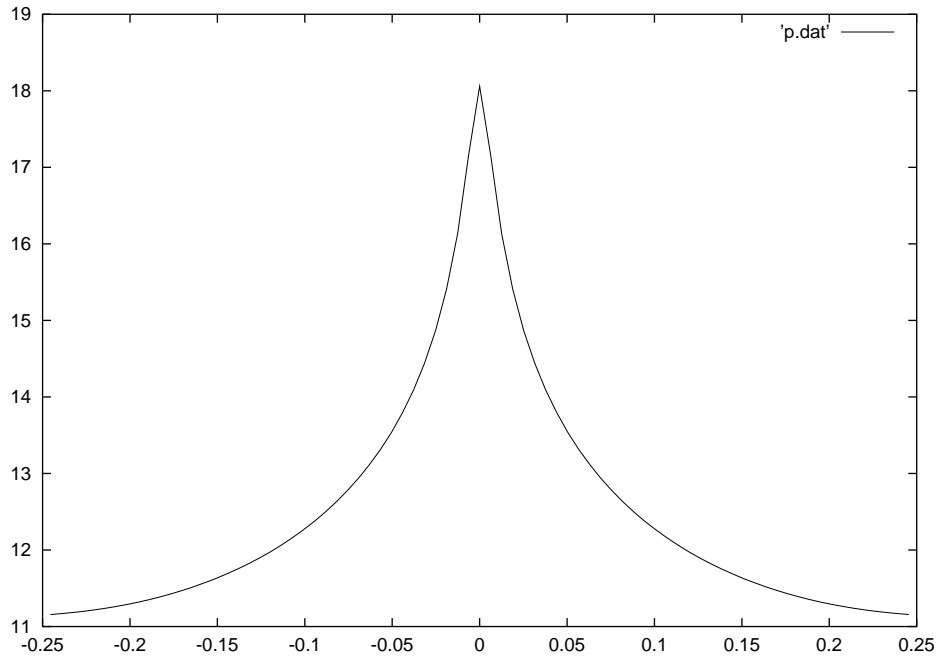
$$A_{,u} = (u + w)^{-1}[CD + (A - B)/2] \quad (12)$$

$$B_{,w} = (u + w)^{-1}[CD + (B - A)/2] \quad (13)$$

$$C_{,u} = (u + w)^{-1}[-AD + (C - D)/2] \quad (14)$$

$$D_{,w} = (u + w)^{-1}[-BC + (D - C)/2] \quad (15)$$

We impose the condition that $P(t, x)$ and $Q(t, x)$ are even functions of x . This insures that $Q_{,x}(t, 0) = 0$ and therefore that the spike will be at $x = 0$. With this condition, we only need to evolve on the domain $x \geq 0$. This corresponds to $u \geq w$. The characteristic initial value formulation for this system is as follows: on a $u = \text{constant}$ surface we give as initial data A and C as functions of w . Equations (13) and (15) are then integrated to yield B and D on the initial data surface. The numerical method used is second order Runge-Kutta. The initial condition for this integration is that $B = A$ and $D = C$ at $u = w$. This is a consequence of the fact that P and Q are even functions of x . Now with A, B, C and D known on the initial surface, equations (12) and (14) can be regarded as ODEs for each value of w . At each grid point, these ODEs are integrated to yield A and C at the next value of u . The numerical method used is a second order predictor-corrector method. This entire process is iterated to produce the full evolution.

FIG. 1: spike in P at $\tau = 9$

We choose the minimum value of w to be zero, corresponding to the light ray that will hit the singularity ($t = 0$) at the center of the spike ($x = 0$). The maximum value of w is the current value of u , corresponding to $x = 0$. Thus as the evolution proceeds, some grid points leave the physical domain and are no longer part of the evolution process. Throughout, we choose $du = dw$. This means that we lose one grid point at each time step. When half of the grid points are lost, we put them back in between the remaining ones and interpolate A and C to obtain their values on the new grid points. Thus we make the grid twice as fine. In this way, as the singularity is approached we always have enough grid points to resolve the ever narrowing spike.

III. RESULTS

While our characteristic method (c-code) allows arbitrary initial data for A and C (as long as the initial data does not determine a Cauchy surface¹), it is helpful to make comparisons with codes using the usual Cauchy methods. We therefore also use codes that evolve equations (2-3) (t-code) and equations (6-7) (τ -code). These codes use standard centered differences for spatial derivatives and the iterated Crank-Nicholson method [15] (ICN) for time evolution. We begin with Cauchy data at $t = \pi$ and evolve using the t-code to $t = \pi/2$. In the course of this evolution, we obtain A and C on the null surface given by $u = \pi/2$ and $0 \leq w \leq \pi/2$, which we use as initial data for the c-code.

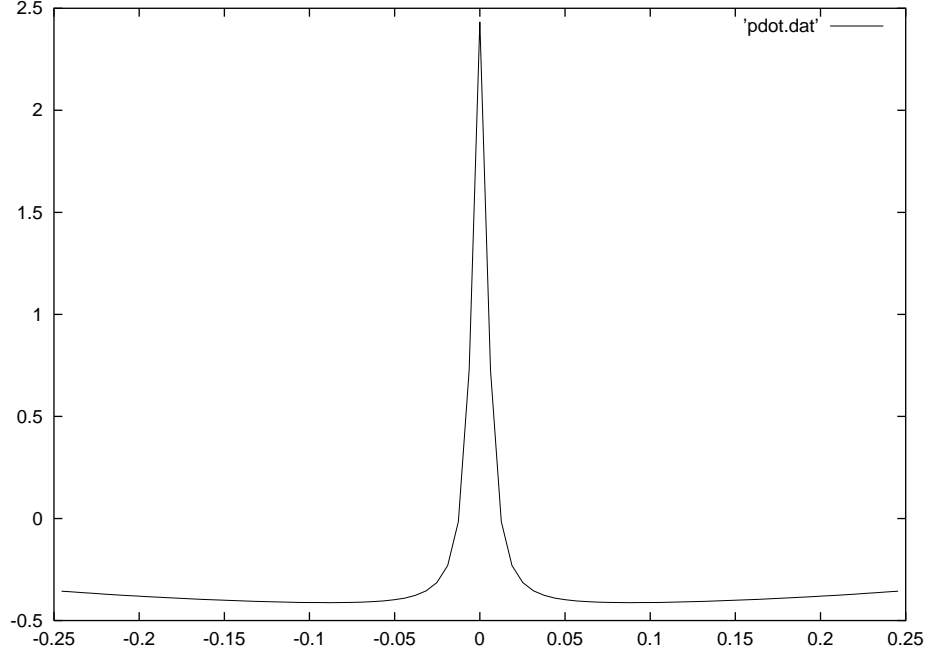
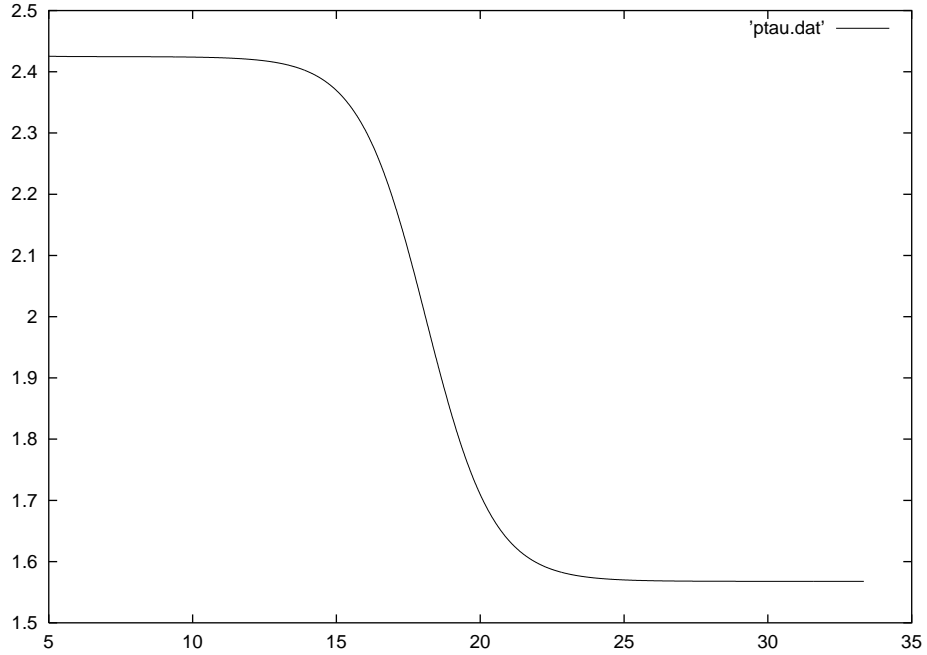
To obtain solutions with high velocity spikes, we note that in the polarized case ($Q = 0$) the velocity can take on any values. We therefore choose initial data with small Q . The form of the data is $P = 0$, $P_{,\tau} = s \cos x$, $Q = q \cos x$ and $Q_{,\tau} = 0$ where s and q are constants. Figures 1 and 2 show the results of evolving these data. Here $s = -8$, $q = 1.0 \times 10^{-3}$ and the result is produced by using the τ -code and evolving to $\tau = 9$.

Now we take the same initial data and evolve it for a longer time, first using the t-code to generate the appropriate initial data for the c-code and then using the c-code to evolve very close to the singularity. The result for $P_{,\tau}$ vs τ at $x = 0$ is shown in figure 3. As the spike forms, $P_{,\tau} > 2$. As the spike narrows, $P_{,\tau}$ decreases, as predicted. Note that $P_{,\tau}$ at the spike starts out larger than 2, and that it is eventually driven below 2.

One might wonder what mechanism is responsible for driving the spike velocity below 2. The answer comes from an examination of equation (6). Rewriting this equation with $P_{,\tau\tau}$ on one side we have

$$P_{,\tau\tau} = e^{-2\tau} P_{,xx} + e^{2P} Q_{,\tau}^2 - e^{2(P-\tau)} Q_{,x}^2 \quad (16)$$

¹ If a Cauchy surface is determined, then the initial data must be compatible with the periodicity of λ .

FIG. 2: spike in $P_{,\tau}$ at $\tau = 9$ FIG. 3: $P_{,\tau}$ at the spike

At the spike the term $e^{2(P-\tau)}Q_{,x}^2$ vanishes and the term $e^{2P}Q_{,\tau}^2$ is positive definite. The term $e^{-2\tau}P_{,xx}$ is negative, since the spike in P is upward pointing. What is happening is that the spike is becoming so narrow and thus $P_{,xx}$ is becoming so large that despite the smallness of $e^{-2\tau}$ the quantity $e^{-2\tau}P_{,xx}$ is not negligible. The term $e^{2P}Q_{,\tau}^2$ is also not negligible, but its magnitude is less than the magnitude of $e^{-2\tau}P_{,xx}$, so $P_{,\tau\tau}$ is negative. In the explicit approximation, $e^{2P}Q_{,\tau}^2$ and $e^{-2\tau}P_{,xx}$ are decaying in magnitude if $P_{,\tau} < 2$, but if $P_{,\tau} > 2$ and if $Q_{,xx}$ does not vanish at the spike they are growing in magnitude, and the leading part of $e^{2P}Q_{,\tau}^2$ is half the magnitude of the leading part of $e^{-2\tau}P_{,xx}$, so the net effect is a decrease in $P_{,\tau\tau}$ [6, 9, 16]. From figure 3 we see that this decrease eventually comes

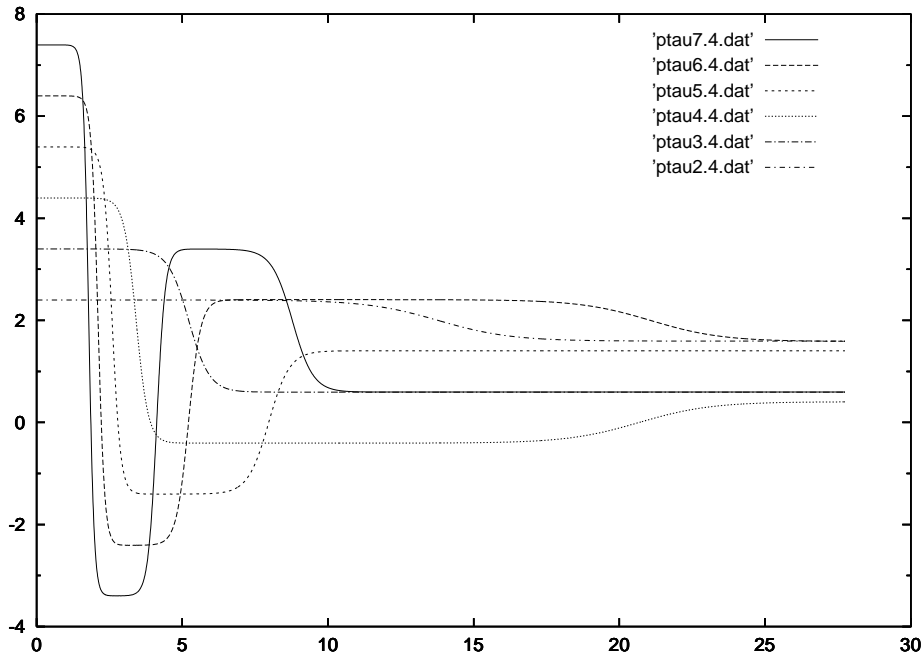


FIG. 4: $P_{,\tau}$ at the spike for different initial values of $P_{,\tau}$.

to an end while $P_{,\tau}$ is still greater than 1. Now the conditions for the explicit approximation of the spike to be valid throughout the approach to the singularity are satisfied, indicating that the spike will persist.

Another family of initial data which we use to generate spikes is $t = t_0$, $P = p$, $P_{,\tau} = s$, $Q = q \cos x$ and $Q_{,\tau} = 0$ where t_0 , p , s and q are constants, with $s > 1$. The constants are chosen so that the explicit approximation to the spike is initially valid, until the spike narrows enough that the velocity begins to slide down. To allow matching of the t-code to the c-code, the value of t_0 is chosen to be $4\pi n/m$, with $n + 1$ the number of grid points for the c-code and the $m + 1$ st grid point identified with the 1st grid point in the t-code (corresponding to a difference in x of 2π). In figures 4-6 we show results from a family of initial data sets with $n = 160$ and $m = 2050$ (which results in $t_0 \approx 0.98$), $p = 0$ and $q = 0.01$. We vary s , from 2.4 to 20.7. In figure 4 we again plot $P_{,\tau}$ vs τ . In figure 5 we plot both $P_{,\tau}$ vs τ and the velocity, v vs τ for a single initial data set, with $s = 13.2$. In figure 6 we plot v vs τ . When $2 < w_0 < 4$ there is just one “slide” in the velocity, v . Its final value is about 4 minus its initial value, and the final value of $P_{,\tau}$ is about equal to $4 - s$. When $4 < s < 6$, there is a slide, after which $P_{,\tau} \approx 4 - s$ (i.e., it is negative), and $v \approx |4 - s|$. After this slide the velocity is approximately constant, while $P_{,\tau}$ “bounces” to a value equal in magnitude to $4 - s$, but now positive ($|4 - s|$). This sort of bounce has been discussed in previous work [6] and is driven by the term $e^{2P} Q_{,\tau}^2$ in the evolution equation for P . When $s > 6$, there is not just one slide in $P_{,\tau}$, but a number of slides. Each slide approximately satisfies the rule $v \rightarrow |4 - v|$ and $P_{,\tau} \rightarrow 4 - P_{,\tau}$. If $P_{,\tau}$ is negative after a slide, then there is a bounce as just described above. If $P_{,\tau} > 2$ after this bounce, then a slide follows, and so on. In each case, finally, $0 < P_{,\tau} < 2$, $P_{,\tau} \approx v$ and the conditions are satisfied such that the explicit approximation of [6] should be valid throughout the remaining approach to the singularity. These results and all other results we obtained from various choices of initial data² agree with the picture we have just presented.

The rule for the final (after all the slides and bounces) value of $P_{,\tau}$, based on the initial value of $P_{,\tau}$ is shown in table I, with $n \geq 0$ an integer, and $0 < \sigma < 1$. Both initially and finally, $v \approx P_{,\tau}$, but this relation does not hold during bounces and slides. The rule for the final value of $P_{,\tau}$ based on the initial value of $P_{,\tau}$ when $Q_{,x} \neq 0$, obtained from the explicit approximations [6] (if $P_{,\tau} > 1$, $P_{,\tau} \rightarrow 2 - P_{,\tau}$ and then if $P_{,\tau} < 0$, $P_{,\tau} \rightarrow -P_{,\tau}$ and reiterate) is also given in the table.³

To obtain a picture of what happens at downward pointing spikes, one could use the same combination t-code

² This method allows study of a large number of different spikes with varied initial conditions into the “asymptotic regime”, since the code runs very quickly.

³ The discussion in this paper assumes “genericity conditions”, for example, that $Q_{,xx} \neq 0$ at upward pointing spikes. For discussion of persistence of high velocity spikes under special conditions, see [9].

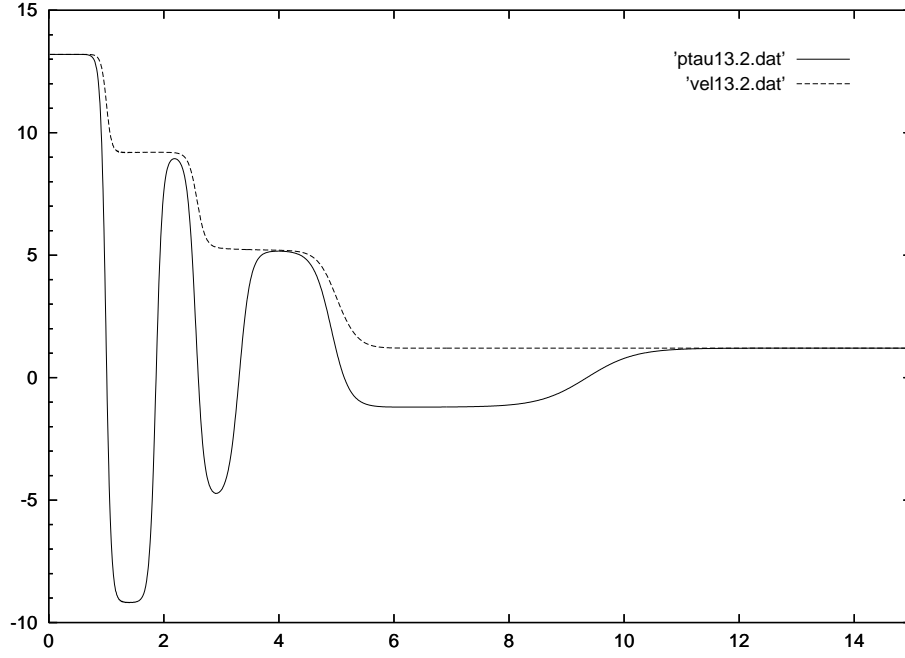


FIG. 5: $P_{,\tau}$ and the velocity at the spike for $P_{,\tau} = 13.2$ initially.

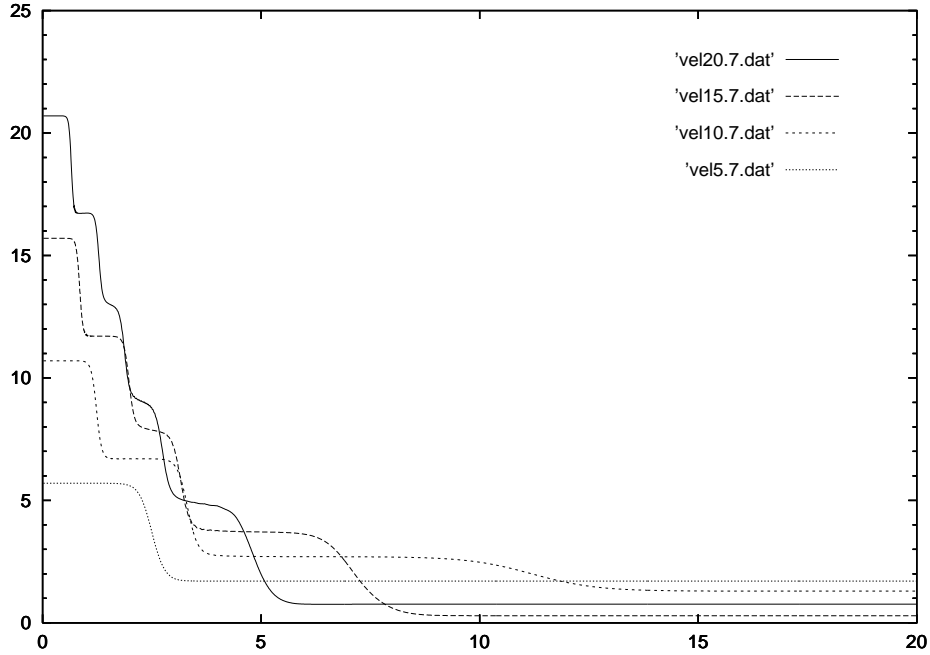


FIG. 6: Velocity at the spike for different initial values $P_{,\tau}$.

and c-code with the appropriate initial data. But this is not necessary, since an upward pointing spike is mapped to a downward pointing spike with $P_{,\tau}^{\text{down}} = 1 - P_{,\tau}^{\text{up}}$ by the Gowdy to Ernst transformation [9]. Thus for downward pointing spikes an *upward* slide in $P_{,\tau}$ occurs if $P_{,\tau} < -1$ at the spike, and the rule for the slide is $P_{,\tau} \rightarrow -P_{,\tau} - 2$. If $P_{,\tau} > 2$ after the slide then there is a *downward* bounce $P_{,\tau} \rightarrow 2 - P_{,\tau}$. Reiterating this until $-1 < P_{,\tau} < 1$, we obtain the rule shown in table II, with $n \geq 0$ and $0 < \sigma < 1$. The Gowdy to Ernst transformation maps the condition $Q_{,x} = 0$ for an upward pointing spike to form to the condition $e^{2P} Q_{,\tau} = 0$ for a downward pointing spike to form.

The c-code only gives us information concerning an extremely small neighborhood of the spike. This is precisely

TABLE I: Final $P_{,\tau}$ from initial $P_{,\tau} > 0$, for integer $n \geq 0$ and $0 < \sigma < 1$.

Initial $P_{,\tau}$	Final $P_{,\tau}$ if $Q_{,x} = 0$	Final $P_{,\tau}$ if $Q_{,x} \neq 0$
$4n + \sigma$	σ	σ
$4n + 1 + \sigma$	$1 + \sigma$	$1 - \sigma$
$4n + 2 + \sigma$	$2 - \sigma$	σ
$4n + 3 + \sigma$	$1 - \sigma$	$1 - \sigma$

TABLE II: Final $P_{,\tau}$ from initial $P_{,\tau} < 0$, for integer $n \geq 0$ and $0 < \sigma < 1$.

Initial $P_{,\tau}$	Final $P_{,\tau}$ if $Q_{,\tau} = 0$	Final $P_{,\tau}$ if $Q_{,\tau} \neq 0$
$-4n - \sigma$	$-\sigma$	σ
$-4n - 1 - \sigma$	$-1 + \sigma$	$1 - \sigma$
$-4n - 2 - \sigma$	σ	σ
$-4n - 3 - \sigma$	$1 - \sigma$	$1 - \sigma$

its advantage. But the rules just obtained raise the question, “How does the small neighborhood of the spike match onto the rest of space when the rule for the final value of $P_{,\tau}$ at the spike agrees with the rule for the final value of $P_{,\tau}$ elsewhere (*i.e.*, in half the cases)?” To see how a spike sits in the rest of the spacetime, we use Cauchy evolution using the symplectic PDE solver [6] with mesh refinement [16]. We use a resolution of 1024 (the 1025th grid point is identified with the 1st, corresponding to a difference in x of 2π). Two levels of mesh refinement are made at spikes, each increasing the resolution five-fold. This code is not as fast as the combination t-code and c-code, and is not as effective over as large of a range of initial data sets nor as far into the asymptotic regime as the combination t-code and c-code. But all the results obtained suggest that when the rule obtained for final value of $P_{,\tau}$ at the spike matches the rule obtained elsewhere, the signatures of the spike are effectively washed out, for both upward and downward pointing spikes. We show an example, for a downward pointing spike, in figure 7. The initial data is $n = 162$ and $m = 2048$ (so $t_0 \approx 0.99$), $s = 5.7$, $p = 0$, $q = 0.01$ and now $Q = q \cos(x + \pi/5)$ so that no spike is at the edge of the grid, for easier implementation of the mesh refinement. $P_{,\tau} \approx -3.7$ when the downward pointing spike begins to form. The spiky features are pronounced in the middle row of figure 7, but by the time of the final row they are disappearing.

IV. CONCLUSIONS

We have seen that there is a mechanism that, in general, eventually drives upward pointing spike velocities below 2 and downward pointing spike velocities below 1. The general asymptotic behavior of Gowdy spacetimes is then that given in [6]. The spacetime is everywhere AVTD. At a set of isolated points there are spikes. The closer a point is to a spike, the longer it takes to reach the VTD regime. Upward pointing spikes in general have $1 < v < 2$, downward pointing spikes in general have $0 < v < 1$ ($-1 < P_{,\tau} < 0$) and the shape of both kinds is described by expressions in [6].

V. ACKNOWLEDGMENTS

This work was partially supported by NSF grant PHY-9988790 to Oakland University and by the Natural Sciences and Engineering Research Council of Canada.

-
- [1] J. Isenberg and V. Moncrief, Ann. Phys. (N.Y.) **199**, 84 (1990).
 - [2] P.T. Chruściel, J. Isenberg and V. Moncrief, Class. Quantum Grav. **7**, 1671 (1990).
 - [3] P.T. Chruściel, Proceedings of the Center for Mathematics and its Applications, **27** (1991).

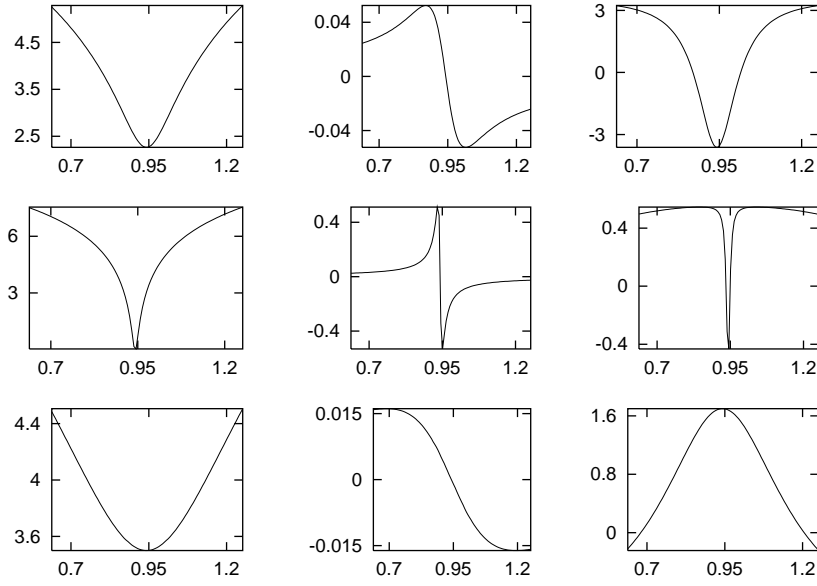


FIG. 7: P vs x (left column), Q vs x (middle column) and $P_{,\tau}$ vs x (right column) at $\tau \approx 3.1$ (top row), $\tau \approx 4.0$ (middle row) and $\tau \approx 6.4$ (bottom row).

- [4] B. Grubišić and V. Moncrief, Phys. Rev. **D47**, 2371 (1993).
- [5] B.K. Berger and V. Moncrief, Phys. Rev. **D48**, 4676 (1993).
- [6] B.K. Berger and D. Garfinkle, Phys. Rev. **D57**, 4767 (1998).
- [7] M. Weaver, J. Isenberg and B.K. Berger, Phys. Rev. Lett. **80**, 2984 (1998).
- [8] A. Rendall, Class. Quantum Grav. **17**, 3305 (2000).
- [9] A. Rendall and M. Weaver, Class. Quantum Grav. **18**, 2959 (2001).
- [10] B.K. Berger, J. Isenberg and M. Weaver, Phys. Rev. **D64**, 084006 (2001).
- [11] H. Elst, C. Uggla and J. Wainwright, Class. Quantum Grav. **19**, 51 (2002).
- [12] H. Ringström, to appear in Mathematical Proceedings of the Cambridge Philosophical Society, gr-qc/0204044.
- [13] R.H. Gowdy, Phys. Rev. Lett. **27**, 826 (1971).
- [14] D. Garfinkle, Phys. Rev. **D51**, 5558 (1995).
- [15] M. Choptuik, in *Deterministic Chaos in General Relativity*, edited by D. Hobill, A. Burd and A. Coley (Plenum, New York, 1994), pp 155-175.
- [16] M. Weaver, Ph.D. Thesis, University of Oregon, 1999.